

# The impact of timing and magnitude of the El Niño-Southern Oscillation on local precipitation levels and temperatures in the Bay Area

Ryan Li<sup>1</sup> and Jian Zhang<sup>2</sup>

<sup>1</sup> Monta Vista High School, Cupertino, California

<sup>2</sup> National Severe Storms Lab, Norman, Oklahoma

## SUMMARY

In this study, we analyzed temperature, Multivariate El Niño-Southern Oscillation Index (MEI), and Standard Precipitation Index (SPI) data from the San Francisco Bay Area from 1971 to 2016. We also analyzed CO<sub>2</sub> records from Mauna Loa, HI for the same time period, along with the annual temperature anomalies for the Bay Area. Understanding the relationships between temperature, MEI, SPI, and CO<sub>2</sub> concentration is important as they measure the major influencers of California's regional climate: temperature, ENSO, precipitation, and atmospheric CO<sub>2</sub>. Thus, measurements of the three variables are key indicators of long term trends in climate, and can reveal the exact effect anthropogenic climate change is having on the Bay Area's climate. Our research question was whether there is a correlation between temperature, MEI, SPI, and atmospheric CO<sub>2</sub> within the Bay Area. We found that there was a clear correlation between warm anomalies and high MEI/low SPI in the period of 2013–2016, however only when both were historically significant. Also, MEI levels in general were highly correlated with temperature, showing that the local temperature anomalies in the Bay Area are significantly influenced by the El Niño-Southern Oscillation (ENSO) cycle. The influence of precipitation on the local temperature anomalies was limited, however. Finally, although there was not a statistically significant link between the atmospheric CO<sub>2</sub> concentration at Mauna Loa, HI and the temperature anomalies in the Bay Area, the consistent increase in CO<sub>2</sub> concentration could have had an impact on the overall increase in annual temperature anomalies from 1971 to 2016.

## INTRODUCTION

The El Niño-Southern Oscillation cycle (ENSO) is a recurring but irregular pattern of oceanic temperatures and atmospheric conditions in the east-central Equatorial Pacific (1), which have large impacts on rainfall and weather patterns in North America. When ENSO is in its “warm” phase (El Niño), warmer than normal ocean temperatures are observed in the Pacific Ocean. Similarly, when ENSO is in its “cold” phase (La Niña), cooler than normal ocean temperatures are seen in the Pacific Ocean (2). In times when ENSO is “neutral”, ocean temperatures in the Pacific Ocean are approximately average (3). ENSO also has a large impact on a global scale, for when

an El Niño or La Niña is present, global temperatures are raised or lowered, respectively (4).

ENSO specifically influences the regional climate within California by shifting the location of the jet stream, which has a large impact on winter weather patterns at mid-latitudes (5). This effect increases the amount of rainfall within the state during the wintertime when an El Niño is present, while decreasing the amount of rainfall during the wintertime when La Niña is occurring (5,6). However, the changes in precipitation patterns within California owing to ENSO are more predictable within Southern California (5,6). If there is neither an El Niño nor a La Niña occurring (ENSO neutral), then other large-scale climate cycles (such as the Arctic Oscillation) have a larger influence on weather patterns within North America (and California) (3). As global temperatures continue to rise, however, the ENSO cycle is expected to have an increasingly greater effect on the temperatures within the southern United States, as well as on global precipitation and temperature (7,8). It is also expected to lead to more extreme droughts and storms globally (8).

The Multivariate ENSO Index (MEI) is used to represent the ENSO cycle within this study. MEI combines several key variables measured in the tropical Pacific basin (30°S–30°N and 100°E–70°W) that reflect the ENSO cycle phenomenon. The variables include the sea surface pressure, sea surface temperature, zonal and meridional components of the surface winds, and cloudiness of the sky (9). Significantly positive or significantly negative annual mean MEI values ( $\geq 0.5$  or  $\leq -0.5$ ) represent warm El Niño or cold La Niña events, respectively.

Another factor which influences California's climate is the amount of precipitation it receives, which can result in drought should lower than normal precipitation levels persist. Drought is defined as the “temporary reduction in water availability below normal quantities” (10), which can be interpreted as an increase in the dryness of an area. Even though California has always had a long history of drought, Diffenbaugh et al. (2015) state in their paper that recently California has had concurrent hot and dry years (11). They go on to say that the probability of this happening in the future will increase, with less precipitation and more evaporation/transpiration resulting from warmer temperatures (11). These conditions can bring about extreme drought events such as the one experienced by California from 2012 to 2016 (10).

The Standard Precipitation Index (SPI) is an index that measures the magnitude of meteorological drought for short

timescales. It is used to quantify measured precipitation as a “standardized departure from a selected probability distribution function that models the raw precipitation data” (12). A larger positive value indicates greater than median precipitation (wetter than normal conditions) while more negative values indicate less than median precipitation (13).

On a larger scale, anthropogenic climate change over the past 150 years has warmed the Earth “at a rate 20-50 times faster” than Earth’s fastest natural climate change events, and its effects have been felt around the world (14). This results in not only habitat loss for plants and animals living within ecosystems globally but also severe infrastructure damage due to more frequent events such as tropical storms, extreme heat events, and disruptions to oceanic circulation which are exacerbated by global warming (15). Yet all of these catastrophic events have occurred when global surface and ocean temperatures have only warmed by approximately 0.85 °C from 1880 to 2012, while by 2100 the global surface temperature is likely to further rise above 1.5 °C relative to what it was in 1880 (16). A major portion of this warming can be directly attributed to human greenhouse gas emissions, specifically CO<sub>2</sub>, which had an exponential growth with “a doubling time of about 30 years since the beginning of the industrial revolution (~1800)” (17).

This study examined whether the local temperatures of the San Francisco Bay Area have a relationship with three factors over the past 46 years: 1) the large-scale ENSO cycle, 2) the Bay Area’s precipitation levels, and 3) the atmospheric CO<sub>2</sub> concentrations. We found that from 2013 to 2016 there was a large correlation between a historically significant high MEI/low SPI and warm annual temperature anomalies within the Bay Area, and that in general the influence of ENSO was a lot stronger than the influence of precipitation on the temperatures within the Bay Area from 1971 to 2016. In addition, from 1971 to 2016, rising annual mean CO<sub>2</sub> concentrations were also correlated with the rise in annual mean temperature anomalies in the Bay Area.

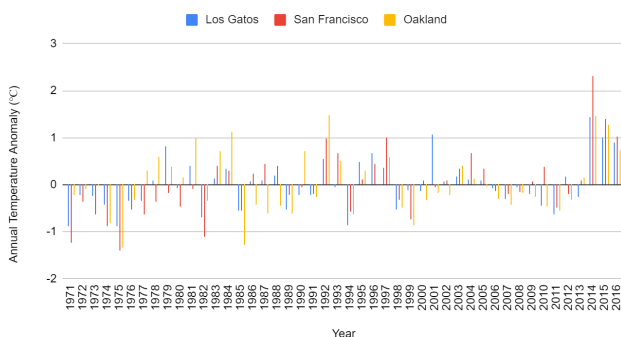


**Fig 1:** Combined annual temperature anomaly vs. year for San Francisco, Los Gatos, and Oakland (1971-2016). In general, negative annual temperature anomalies are observed towards the start of the study period, while positive annual temperature anomalies are observed towards the end of the study period. There is a large increase in the annual temperature anomaly from 2013 to 2014 across all three locations, with positive temperature anomalies persisting for all three locations until the end of the study period (2016).

## RESULTS

To determine the trend in temperature fluctuations within the Bay Area over a 46-year period, we calculated and analyzed the annual temperature anomalies in three locations in the Bay Area: San Francisco, Los Gatos, and Oakland. From 1971 to 2016, we observed a large spike in the annual temperature anomaly in 2014, with Los Gatos, San Francisco, and Oakland possessing temperature anomalies of 1.4 °C, 2.3 °C, and 1.5 °C, respectively (**Fig. 1**). We then performed a paired t-test on the average monthly high/low temperatures in 2014 in all three locations against the 1971–2016 average to determine the significance of the temperature increase (**Table 1**). Paired t-test results showed that the average monthly temperatures in 2014 all had *p*-values below the 0.05 threshold, rendering the temperature anomalies significant in the historical context (**Table 1**).

	SF (High)	SF (Low)	Los Gatos (High)	Los Gatos (Low)	Oakland (High)	Oakland (Low)
Paired t-test results:	<0.0001	<0.0001	0.0001	0.003	0.0011	0.0035

**Table 1:** Paired t-test results for average monthly high/low temperature in 2014 vs. the 1971-2016 mean (San Francisco, Los Gatos, and Oakland). All of the *p*-values calculated are below the statistical significance threshold (*p*=0.05), meaning the 2014 temperature anomalies are significant in the historical context.

In order to better visualize the average warming over the 46-year period for each individual city, the annual temperature anomalies for each station were placed in three separate graphs, and trendlines were generated by Google Sheets for each graph (**Fig. 2**). An example of San Francisco’s annual temperature anomaly bar graph along with its trendline is shown in **Figure 2A**. There was a warming trend observed in San Francisco, Los Gatos, and Oakland from 1971 to 2016, with the average warming (measured using the endpoints of each cities’ annual temperature anomaly trendline) being 1.34 °C, 0.63 °C, and 0.32 °C, respectively (**Fig. 2**). By averaging these values, the average warming for the Bay Area from 1971 to 2016 was found to be 0.76 °C.

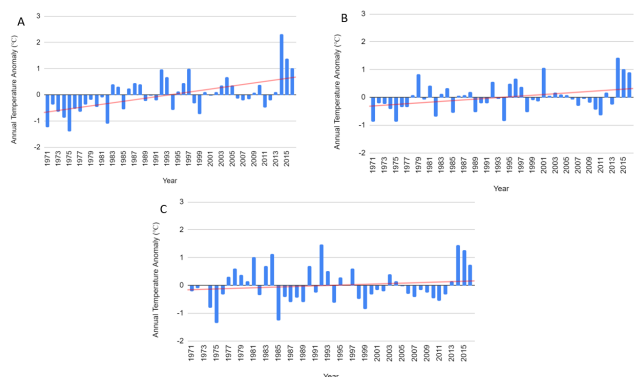


**Fig 2:** Annual temperature anomaly vs. year for San Francisco (A), Los Gatos (B), and Oakland (C) with trendlines (1971-2016). The trendlines depict an increasing annual temperature anomaly across all three locations within the study period. A large increase in annual temperature anomaly from 2013 to 2014 is also seen in all three locations, with positive temperature anomalies persisting for all three locations until the end of the study period (2016).

The relationship between Bay Area annual temperature anomaly (Ta), annual mean MEI, and annual mean SPI on both a short and long timescale was examined by plotting the three variables onto one graph, along with their three-year moving averages (Fig. 3). The first two variables showed a large positive correlation ( $r = 0.73$  between the three-year moving averages of Ta and MEI), with Ta trailing MEI until 1997, after which the MEI began trailing Ta (Fig. 3). For the individual annual data points, the correlation coefficient  $r$  was lower, equaling 0.53 between Ta and MEI (Fig. 3). Ta showed somewhat of an inverse correlation with SPI ( $r = -0.17$  between the three-year moving averages of Ta and SPI), becoming the most pronounced in the period after 2009. The correlation coefficient for the individual data points between Ta and SPI was also lower than their three-year moving averages, equating to  $-0.05$ . From 2013 to 2016, there was a clear spike then gradual decrease in Ta which exceeded its fluctuations during the entire 1971–2016 period, the SPI decreased to record lows historically, and the MEI crossed the 0.5 El Niño threshold on a steep ascending trend.

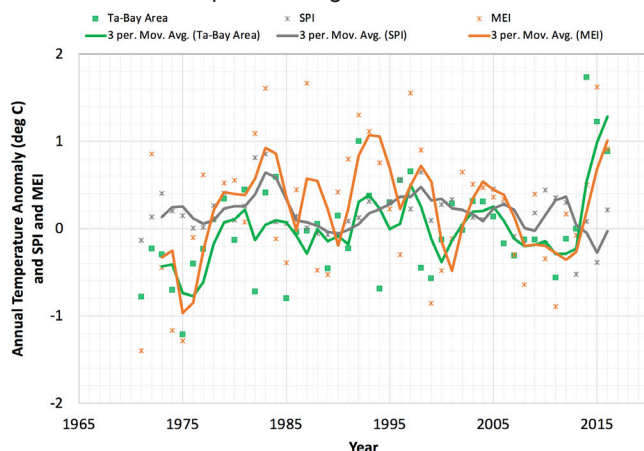


**Fig 3:** Bay Area annual temperature anomaly (1971-2016, green squares), annual mean SPI (1971-2016, grey stars), and annual mean MEI (1971-2016, orange stars) and their corresponding three-year moving averages (green, grey, and orange solid lines, respectively). A large increase in both Ta and MEI from 2013-2014 is seen, and both variables were positive from 2014 to 2016. Meanwhile, a large decrease in SPI is observed in both 2013 and 2015.

To observe the correlation between Ta and annual mean CO<sub>2</sub> concentration, the two variables were plotted onto one graph (Fig. 4). We noticed a steady rise in CO<sub>2</sub> concentration between 1971 and 2016. There was a strong ( $R^2 > 0.99$ ) trend of CO<sub>2</sub> increase at  $\sim 1.73$  ppm/year, while the Ta also showed a trend of increase at  $\sim 0.03$  deg/year but with a lower  $R^2$  value (0.157, Fig. 4).

## DISCUSSION

Our research question concerned the relationship between temperature, MEI, SPI, and atmospheric CO<sub>2</sub> from 1971 to 2016 in the San Francisco Bay Area. Annual temperature anomalies for the three cities (San Francisco, Los Gatos, Oakland) as well as for the Bay Area were derived

from monthly high/low averages in this time period, annual mean MEI data was converted from bimonthly data, annual mean SPI was converted from monthly averages, and annual mean CO<sub>2</sub> was converted from monthly averages. A paired t-test was performed on the 2014 warm temperature anomaly data in order to determine if it was statistically significantly warmer than the average temperature anomaly baseline over the entire study period, the trendlines in Figure 2 helped to quantify the growth in each of the three cities' annual temperature anomalies from 1971 to 2016, and the three-year moving averages in Figure 3 helped to create a more accurate representation of the long term trends of Ta, MEI, and SPI by eliminating short term variabilities.

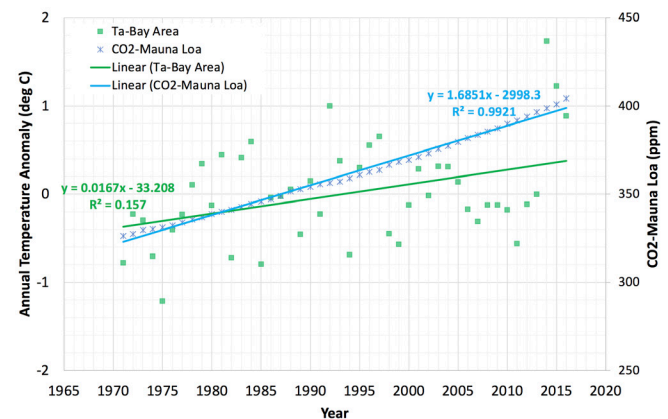


**Fig 4:** Bay Area annual temperature anomaly (1971-2016, green squares and solid line) and Mauna Loa, HI annual mean CO<sub>2</sub> (1971-2016, blue stars and solid line). Annual mean CO<sub>2</sub> increased linearly within the study period, with the correlation coefficient  $R^2$  being 0.9921. Ta also increased within the study period but with a lower  $R^2$  (0.157).

During the 2014 temperature spike and the 2013–2016 warm period, the Bay Area annual mean MEI crossed over the 0.5 threshold, which indicates an El Niño event, as Ta jumped above historic levels; however this relationship wasn't significant, as previous periods including 1981–1983, 1985–1987, and 1989–1992 had annual mean MEI levels at or exceeding 2013 to 2016's levels without a similar spike in Ta (Fig. 3). In addition, the relatively high MEI levels from 1981 to 1983 was also paired with a record SPI increase from 0.26 to 0.86 from 1981 to 1983. This positive correlation between the MEI and SPI could be explained by the fact that the El Niño (larger MEI values) brought more precipitation to the Bay Area, reflected by the relatively large positive SPI values. However, as the MEI increased from 1985 to 1987 and 1989–1992, the SPI was always between  $-0.2$  and  $0.2$ , indicating that there wasn't an increase in precipitation levels concurrent with the El Niños during these time periods. Taken together, the behavior of the MEI and SPI during the four periods of time (1981–1983, 1985–1987, 1989–1992, 2013–2016) verifies the claim made by the University of California Museum of Paleontology and Tom Di Liberto that the exact effect which ENSO has on precipitation levels in Northern

California is highly variable (5,6). In addition, it is seen that a high MEI alone does not necessarily directly correlate year to year with large warm temperature anomalies ( $r = 0.53$ ), but it is still worth noting the relatively high correlation coefficient ( $r = 0.73$ ) between these two variables on a three-year moving average, indicating that the MEI has a relatively large-scale influence overall on  $T_a$  within the Bay Area.

The Bay Area annual mean SPI values from 2013 to 2016 provided another piece of the puzzle for the temperature spike. During this time the SPI dropped to two of the lowest values observed within the 46-year study period (-0.52 and -0.39) in 2013 and 2015 respectively (**Fig. 3**), rendering it historically significant. This also shows that it was the driest period over the 46 years studied. The historical drought combined with the warming El Niño trend may have been a main contributor to the historic warm  $T_a$  (**Fig. 3**). The SPI itself, however, did not show a strong correlation with  $T_a$  given the fact that the correlation coefficient between the three-year moving averages of SPI and  $T_a$  was -0.17 and that there was an even smaller correlation coefficient between the annual averages ( $r = -0.05$ ).

Overall, the 2014–2016 historically high  $T_a$  in conjunction with the historically low Bay Area annual mean SPI, both of which had simultaneous magnitudes which were not otherwise seen during the 46-year time period analyzed in this study, support Diffenbaugh et al. (2015)'s claim that rising temperatures increase the likelihood of extreme dry conditions and warm temperatures coinciding with each other (11). However, this relationship seems variable, as the relationship between precipitation and  $T_a$  was rather weak ( $r = -0.05$  without the three-year moving average and  $r = -0.17$  with the three-year moving average). Also, there seems to be a pattern of severe droughts concurrent with warm El Niño resulting in significant warm anomalies, such as the ones observed from 2013 to 2016. In addition, ENSO (with a three-year moving average) had an overall large observed impact on the three-year moving average  $T_a$ , while SPI possessed a weak impact on both the year-to-year and the three-year moving average  $T_a$ . These results indicate that the Bay Area temperature is significantly influenced by the oceanic system and that this influence could be on a multi-year scale, while the relationship between precipitation and temperature anomalies is not as coherent (**Fig. 3**). In addition, we concluded that ENSO's effect on precipitation within the Bay Area is variable.

The annual mean  $CO_2$  concentration at Mauna Loa showed a persistent increase between 1971 and 2016 (**Fig. 4**). While there was no  $CO_2$  spike corresponding to the 2014  $T_a$  spike, the upward trend of  $CO_2$  concentration may still explain the overall increase in the annual average temperature and  $T_a$  during the study period (**Fig. 4**) through its role as a greenhouse gas. Thus, the overall average increase of 0.76 °C in the Bay Area may be attributed to the  $CO_2$ -induced greenhouse effect; however, it is still important to remember that other properties such as evaporative cooling levels

and energy storage capacity also have an impact on local temperatures in addition to incoming and outgoing solar radiation.

The next steps for this research include incorporating more data series for both temperature and SPI for additional cities in the Bay Area to ensure that the results are truly representative of the Bay Area, as well as extending the time period examined to further reduce potential bias which may be present in the current study period. An examination of the impacts that droughts may impose on Northern California ecosystems would allow us to better understand the current situation of both urban ecosystems within the Bay Area as well as the coniferous forests which dominate the Northern Californian landscape, including how much of an effect rising temperatures and increasing droughts in the future will have on the health of these ecosystems.

## MATERIALS AND METHODS

In this study we focused on the San Francisco Bay Area (located in Northern California), specifically the three cities of San Francisco, Los Gatos, and Oakland, CA. The time period that was selected spanned from 1971 to 2016, encompassing the period of the 2012–2016 extreme drought in California as well as the forty years preceding the unprecedented warm and dry period. Three weather stations, one from each of these cities, with the most complete temperature records were selected, and monthly average high ( $T_h$ ) and low ( $T_l$ ) temperatures from each of these three stations were recorded on a spreadsheet. This data was provided by the National Centers for Environmental Information (NCEI) of National Oceanic and Atmospheric Administration (NOAA) through their Climate Data Online tool (18).

The monthly average high and low temperatures reflected the mean fluctuation between the daily high and low temperature in the month for each station. For our study, such small-scale fluctuations had to be filtered out to help reveal any long-term trend in the temperature data. Therefore, annual temperature anomalies ( $T_a$ ) for all three locations were calculated using Equation (1) below:

$$T_a(j) = T_y(j) - T_b \quad (1)$$

Here  $j$  represents the year and ranges from 1971 to 2016,  $T_y$  represents the average annual temperature for each year, and  $T_b$  represents the 46-year mean temperature.  $T_b$  was calculated based on Equation (2) below:

$$T_b = \sum_{j=1971}^{2016} T_y(j)/46 \quad (2)$$

And  $T_y$  was calculated based on Equation (3):

$$T_y(j) = \sum_{i=1}^{12} T_m(i)/12 \quad (3)$$

where  $i$  represents the month and ranges from 1 to 12 and  $T_m$  represents the average monthly temperature and was defined as follows:

$$T_m(i) = [T_h(i) + T_l(i)]/2 \quad (4)$$

By calculating the average of the monthly high and low temperatures (Eq. 4), the diurnal variabilities were removed in the monthly mean temperature ( $T_m$ ). Calculating the average of the monthly mean over the year (Eq. 3) further removed seasonal variabilities in the annual mean temperature ( $T_y$ ) and subsequently the annual temperature anomaly ( $T_a$ ). By using  $T_a$  instead of monthly temperature anomalies, potential climate-related trends can be better presented.  $T_a$  was then converted into units of °C to ensure consistency and was used for the remainder of this study. In addition, a paired t-test was performed on the average monthly high/low temperatures in all three locations for 2014 against the 1971–2016 average to determine the significance of the temperature increase (Table 1).

The endpoints of each trendline (which was generated along with the graphs in Google Sheets) were used to calculate the magnitude of warming for each of the three locations (Fig. 2). The three warming magnitudes were then averaged to represent the average warming in the Bay Area. Afterwards, the annual temperature anomalies for all three stations were averaged to get  $T_a$ , which was more representative of the Bay Area's regional climate.

Next, bi-monthly data of the MEI (9) for 1971–2016, supplied by the NOAA Physical Sciences Laboratory (19), was placed on another spreadsheet. The bi-monthly MEIs were then averaged for each year to obtain the annual mean MEI.

In addition, monthly SPI (13) data for each of the three stations for the period 1971–2016 was taken from the Climate.gov's Drought Risk Atlas (20), then averaged to obtain the annual mean SPI for the Bay Area. This ensured that annual averages were present throughout all of the datasets. Then  $T_a$ , annual mean MEI, and annual mean SPI were plotted onto the same continuous graph (Fig. 3). A three-year moving average was applied to all three data sets to smooth out some short-term natural variabilities and to help better visualize any long-term trends and relationships in the data.

Finally, monthly average atmospheric CO<sub>2</sub> concentration (ppm) from Mauna Loa, HI, which also spanned from 1971 to 2016, was imported onto a spreadsheet. This data was provided by the Scripps CO<sub>2</sub> Program (21). Since CO<sub>2</sub> tends to be well mixed when it is emitted into the atmosphere globally (22), the concentrations of the gas measured at

Mauna Loa would therefore be representative of the levels within the Bay Area on the annual scale. The annual mean CO<sub>2</sub> concentrations were calculated using Equation (5):

$$C_y(j) = \sum_{i=1}^{12} C_m(i)/12 \quad (5)$$

where  $i$  represents the month, and ranges from 1–12 and  $C_m$  represents the monthly average CO<sub>2</sub> concentration. CO<sub>2</sub> concentrations were placed into a continuous graph with  $T_a$  (Fig. 4).

#### ACKNOWLEDGEMENTS

I would like to thank Spencer Eusden and Daniel Dudek for creating and running the Monday and Tuesday lectures for the Headwaters Science Institute, as well as being available for advice on designing our projects and writing our research papers during the office hour sessions. I would also like to acknowledge the Headwaters Science Institute for providing me with this opportunity to not only meet my knowledgeable mentor but also for me to experience the scientific research process and write my first research paper.

**Received:** August 17, 2020

**Accepted:** April 15, 2021

**Published:** May 9, 2021

#### REFERENCES

- NOAA. "What are El Niño and La Niña?" *National Ocean Service Website*, 10 Feb 2020, oceanservice.noaa.gov/facts/ninonina.html.
- "What is La Niña?" *PMEL*, Accessed 27 Nov 2020, www.pmel.noaa.gov/el\_nino/what-is-la-nina.
- Becker, Emily. "September 2019 ENSO update: feeling neutral." *Climate.gov*, 12 Sep 2019, www.climate.gov/news-features/blogs/enso/september-2019-enso-update-feeling-neutral.
- Pidcock, Roz. "Interactive: How much does El Niño affect global temperature?" *CarbonBrief*, 20 Jan 2017, www.carbonbrief.org/interactive-much-el-nino-affect-global-temperature.
- "El Niño." *UCMP*, Accessed 27 Nov 2020, ucmp.berkeley.edu/education/dynamic/session4/ sess4\_hydroatmo3.htm.
- Liberto, Tom Di. "Why did it rain so much in California during last year's La Niña?" *Climate.gov*, 26 Jan 2018, www.climate.gov/news-features/blogs/enso/why-did-it-rain-so-much-california-during-last-year%E2%80%99s-la-ni%C3%B1a.
- Liberto, Tom Di. "Changes in ENSO impacts in a warming world." *Climate.gov*, 27 Sep 2018, www.climate.gov/news-features/blogs/enso/changes-enso-impacts-warming-world.
- E360 Digest. "Climate Change is Making El Niños More Intense, Study Finds." *Yale Environment 360*, 23 Oct 2019, e360.yale.edu/digest/climate-change-is-making-el-ninos-

more-intense-study-finds.

9. Wolter, Klaus, and Michael S. Timlin. "Monitoring ENSO in COADS with a seasonally adjusted principal component index." *Proc. of the 17th Climate Diagnostics Workshop*, Norman, OK, NOAA/NMC/CAC, NSSL, Oklahoma Clim. Survey, CIMMS and the School of Meteor., Univ. of Oklahoma, 1993, pp. 52-57. Available at: [www.psl.noaa.gov/enso/mei.old/WT1.pdf](http://www.psl.noaa.gov/enso/mei.old/WT1.pdf).

10. Lund, Jay, et al. "Lessons from California's 2012–2016 Drought." *J. of Water Resources Planning and Management*, Vol. 144, Issue 10, 2018. [ascelibrary.org/doi/full/10.1061/\(ASCE\)29WR.1943-5452.0000984](https://doi.org/10.1061/(ASCE)29WR.1943-5452.0000984).

11. Diffenbaugh, Noah S., et al. "Anthropogenic warming has increased drought risk in California." *PNAS*, 112 (13): 3931–3936, 2015. [doi.org/10.1073/pnas.1422385112](https://doi.org/10.1073/pnas.1422385112).

12. Keyantash, John, & National Center for Atmospheric Research Staff (Eds). "The Climate Data Guide: Standardized Precipitation Index (SPI)." *Climate Data Guide*, 07 Aug 2018. [climatedataguide.ucar.edu/climate-data/standardized-precipitation-index-spi](https://climatedataguide.ucar.edu/climate-data/standardized-precipitation-index-spi).

13. "Explanation of Standard Precipitation Index (SPI)." *Indiana Department of Natural Resources*, Accessed 27 Nov 2020, [www.in.gov/dnr/water/4864.htm](http://www.in.gov/dnr/water/4864.htm).

14. Nuccitelli, Dana. "New report finds costs of climate change impacts often underestimated." *Yale Climate Connections*, 18 Nov 2019, [www.yaleclimateconnections.org/2019/11/new-report-finds-costs-of-climate-change-impacts-often-underestimated/](http://www.yaleclimateconnections.org/2019/11/new-report-finds-costs-of-climate-change-impacts-often-underestimated/).

15. "The missing economic risks in assessments of climate change impacts." *The London School of Economics and Political Science*, 20 Sept 2019, [www.lse.ac.uk/GranthamInstitute/publication/the-missing-economic-risks-in-assessments-of-climate-change-impacts/](http://www.lse.ac.uk/GranthamInstitute/publication/the-missing-economic-risks-in-assessments-of-climate-change-impacts/).

16. Core Writing Team, Rajendra K. Pachauri and Leo Meyer (eds.). "Climate Change 2014: Synthesis Report. Contribution of Working Groups I, II and III to the Fifth Assessment Report of the Intergovernmental Panel on Climate Change." *IPCC*, Geneva, Switzerland, 2014, 151 pp. [www.ipcc.ch/report/ar5/syr/](http://www.ipcc.ch/report/ar5/syr/).

17. Hofmann, David, J. Butler, P. Tans. "A new look at atmospheric carbon dioxide." *Atmospheric Environment*, 2009. 10.1016/j.atmosenv.2008.12.028. [www.sciencedirect.com/science/article/abs/pii/S1352231008011540](http://www.sciencedirect.com/science/article/abs/pii/S1352231008011540).

18. "Climate Data Online." *NCEI, NOAA*, Accessed 24 Mar 2021, [www.ncdc.noaa.gov/cdo-web/](http://www.ncdc.noaa.gov/cdo-web/).

19. "MEI Index." *PSL, NOAA*, Accessed 24 Mar 2021, [www.psl.noaa.gov/enso/mei.old/table.html](http://www.psl.noaa.gov/enso/mei.old/table.html).

20. "Climate Data." *Drought Risk Atlas*, Accessed 24 Mar 2021, [droughtatlas.unl.edu/Data/Climate.aspx](http://droughtatlas.unl.edu/Data/Climate.aspx).

21. "Atmospheric CO<sub>2</sub> Data." *Scripps Institution of Oceanography*, Accessed 24 Mar 2021, [scrippsco2.ucsd.edu/data/atmospheric\\_co2/primary\\_mlo\\_co2\\_record.html](http://scrippsco2.ucsd.edu/data/atmospheric_co2/primary_mlo_co2_record.html).

22. "6 things to know about carbon dioxide." *Earthsky*, 20 July 2019, [earthsky.org/earth/6-things-to-know-carbon-dioxide-co2-greenhouse-gas](http://earthsky.org/earth/6-things-to-know-carbon-dioxide-co2-greenhouse-gas).

**Copyright:** ©2021 Li and Zhang. All JEI articles are distributed under the attribution non-commercial, no derivative license (<http://creativecommons.org/licenses/by-nc-nd/3.0/>). This means that anyone is free to share, copy and distribute an unaltered article for non-commercial purposes provided the original author and source is credited.